Int J Clin Exp Pathol 2014;7(1):301-312
www.ijcep.com /ISSN:1936-2625/IJCEP1311042

Original Article

Expression of metabolism-related proteins in triple-negative breast cancer

Min-Ju Kim, Do-Hee Kim, Woo-Hee Jung, Ja-Seung Koo

Department of Pathology, Severance Hospital, Brain Korea 21 PLUS Project for Medical Science, Yonsei University College of Medicine, Seoul, South Korea

Received November 18, 2013; Accepted December 12, 2013; Epub December 15, 2013; Published January 1, 2014

Abstract: To investigate the dominant metabolic type of triple-negative breast cancer (TNBC) and evaluate its clinical implication through analysis of protein expression related to glycolysis, glutaminolysis, and mitochondrial oxidative phosphorylation. Tissue samples from 129 patients with TNBC who underwent mastectomy due to invasive breast cancer from 2000 to 2005 were prepared for tissue microarray. By immunohistochemical staining of the tissue microarrays, the markers of glycolysis-related proteins (Glut-1, CAIX, MCT4), glutaminolysis-related proteins (GLS1, GDH, ASCT2), and mitochondrial enzymes (ATP synthase, SDHA and SDHB) were analyzed. Based on the results, the metabolic phenotypes were defined based on positivity for more than two of three markers for each phenotype as follows: glycolysis type (Glut-1, CAIX and MCT4), glutaminolysis type (GLS1, GDH and ASCT2) and mitochondrial type (ATP synthase, SDHA and SDHB). The percentages of samples with metabolic phenotypes of tumor and stroma of TNBC were as follows: for tumor, mitochondrial type (85.3%) > glutaminolysis type (67.4%) > glycolysis type (63.0%); and for stroma, glutaminolysis type (37.2%) > glycolysis type (16.3%) > mitochondrial type (14.0%). The most common metabolic phenotype of TNBC was glycolysis type for basal-like type and non-glycolysis type for non-basal-like type ($p=0.047$). The correlation between glutaminolysis and mitochondrial type was statistically significant in both tumor and stroma ($p<0.001$). In conclusion, tumor cells of TNBC express glycolysis and mitochondrial metabolism-related proteins. Glycolysis type is the most common phenotype of basal-like type, and reversely, non-glycolysis type is the most common phenotype of non basal-like type.

Keywords: Breast, glycolysis, glutaminolysis, mitochondria, triple-negative breast cancer

Introduction

Breast cancer is one of the most heterogeneous tumors in terms of clinical behavior, outcome and treatment response. Consistent efforts are necessary to classify heterogeneous breast cancer. One approach has been gene profiling studies, which classify breast cancer into five subtypes with distinct molecular signatures and clinical implications: normal breast-like, luminal A, luminal B, HER-2, and basal-like phenotypes [1, 2]. Aside from these five subtypes, breast cancer negative for estrogen receptor (ER), progesterone receptor (PR) and HER-2 is defined as triple-negative breast cancer (TNBC) [3]. As TNBC is negative for these receptors, there is no effective targeted therapy, and the tumor is heterogeneous. TNBC can be classified into basal-like (39-54%), molecular apocrine (25-39%), or claudin-low (7-14%) based on gene profiling [4]. The general characteristics of TNBC include high histologic grade, increased mitosis, tumor necrosis, aggressive tumor behavior, and poor prognosis [5-8], which are very similar to the features of tumors with high metabolic activity. The crucial components of tumor metabolism include glycolysis, glutaminolysis, and mitochondrial oxidative phosphorylation [9], and the important proteins for each metabolic component are summarized in **Table 1**. Previous studies have reported that the dominant metabolism of tumors can vary according to the tumor type [9, 10]. As TNBC is a heterogeneous tumor, variability in dominant metabolism is expected, but few studies have been conducted. The objective of this study was to investigate the dominant metabolic type of TNBC through the analy-

Table 1. Key proteins in cancer metabolism

Category	Function
Glycolysis-related	
Glut-1	Transports glucose into cells
CAIX	Neutralizes lactate-induced acidification during glycolysis
MCT4	Transports lactate produced by glycolysis out of cells
Glutaminolysis-related	
GLS1	Converts glutamine to glutamate
GDH	Converts glutamate to α-ketoglutarate
ASCT2	Transports glutamine into cells
Mitochondrial metabolism-related	
ATP synthase	Synthesizes ATP from ADP in mitochondria
SDHA	A component of respiratory complex II in mitochondria; oxidates succinate to fumarate during the citric acid cycle
SDHB	A component of respiratory complex II in mitochondria; oxidates succinate to fumarate during the citric acid cycle

CAIX, carbonic anhydrase IX, MCT, monocarboxylate transporter, GLS, glutaminase, GDH, Glutamate dehydrogenase, ASCT2, ASC-like Na(+)-dependent neutral amino acid transporter, SDH, Succinate dehydrogenase.

sis of protein expression associated with glycolysis, glutaminolysis and mitochondrial oxidative phosphorylation and to elucidate the implications of our findings.

Materials and methods

Patient selection

The subjects of this study included patients with TNBC who underwent mastectomy after the diagnosis of breast cancer in Yonsei University Severance Hospital from January 2000 to December 2005. The patients who received hormone therapy or chemotherapy prior to the surgery were excluded. This study was approved by the Institutional Review Board of Yonsei University Severance Hospital. TNBC was defined as ER-, PR- and HER-2-negative as determined by immunohistochemistry (IHC) and by fluorescence *in situ* hybridization (FISH). A cut-off value of 1% or more positively stained nuclei was used to define ER and PR positivity [11]. HER-2 staining was analyzed according to the American Society of Clinical Oncology (ASCO)/College of American Pathologists (CAP) guidelines using the following categories: 0=no immunostaining; 1^+=weak incomplete membranous staining, less than 10% of tumor cells; 2^+=complete membranous staining, either uniform or weak in at least 10% of tumor cells; and 3^+=uniform intense membranous staining in at least 30% of tumor cells [12]. HER-2 immunostaining was considered positive when strong (3^+) membranous staining was observed, whereas cases with 0 to 1^+ were regarded as negative. The cases showing 2^+ HER-2 expression were evaluated for HER-2 amplification by FISH. All the cases were retrospectively reviewed by a breast pathologist (Koo JS), and histological analysis was conducted with hematoxylin and eosin (H&E)-stained slides. The histological grade was assessed using the Nottingham grading system [13]. Clinicopathologic parameters evaluated in each case included patient age at initial diagnosis, lymph node metastasis, tumor recurrence, distant metastasis, and patient survival.

Tissue microarray

On H&E-stained slides of tumors, a representative area was selected, and the corresponding spot was marked on the surface of the paraffin block. Using a biopsy needle, the selected area was punched out, and a 3-mm tissue core was placed into a 6 × 5 recipient block. The tissue of the invasive tumor was extracted. More than two tissue cores were extracted to minimize the extraction bias. Each tissue core was assigned with a unique tissue microarray location number that was linked to a database containing other clinicopathologic data.

Immunohistochemistry

The antibodies used for immunohistochemistry in this study are shown in **Table 2**. All the immu-

Table 2. Clone, dilution, and source of antibodies used

Antibody	Clone	Dilution	Company
Molecular phenotype-related			
Basal-like-related			
Cytokeratin 5/6	D5/16B4	1:50	DAKO, Glostrup, Denmark
EGFR	EGFR.25	1:50	Novocastra, Newcastle, UK
Claudin-low-related			
Claudin 3	Polyclonal	1:50	Abcam, Cambridge, UK
Claudin 4	Polyclonal	1:100	Abcam, Cambridge, UK
Claudin 7	Polyclonal	1:100	Abcam, Cambridge, UK
E-cadherin	36B5	1:100	Novocastra, Newcastle, UK
Molecular apocrine-related			
Androgen receptor	AR441	1:50	DAKO, Glostrup, Denmark
GGT1	IgG2A	1:50	Abcam, Cambridge, UK
Immune-related			
STAT1	Polyclonal	1:100	Abcam, Cambridge, UK
IL-8	807	1:50	Abcam, Cambridge, UK
Proliferation-related			
Ki-67	MIB-1	1:150	DAKO, Glostrup, Denmark
Metabolic phenotype-related			
Glycolysis-related			
Glut-1	SPM498	1:200	Abcam, Cambridge, UK
CAIX	Polyclonal	1:100	Abcam, Cambridge, UK
MCT4	Polyclonal	1:100	Santa Cruz, CA, USA
Glutaminolysis-related			
GLS1	Polyclonal	1:50	Abcam, Cambridge, UK
GDH	Polyclonal	1:100	Abcam, Cambridge, UK
ASCT2	Polyclonal	1:100	Abcam, Cambridge, UK
Mitochondrial metabolism-related			
ATP synthase	15H4C4	1:100	Abcam, Cambridge, UK
SDHA	2E3GC12FB2AE2	1:100	Abcam, Cambridge, UK
SDHB	21A11AE7	1:100	Abcam, Cambridge, UK

EGFR, epidermal growth factor receptor, GGT1, gamma-glutamyltransferase 1, STAT1, Signal Transducers and Activators of Transcription1, IL, interleukin, CAIX, carbonic anhydrase IX, MCT, monocarboxylate transporter, GLS, glutaminase, GDH, Glutamate dehydrogenase, ASCT2, ASC-like Na(+)-dependent neutral amino acid transporter, SDH, Succinate dehydrogenase.

nohistochemical assays were conducted with formalin-fixed, paraffin-embedded tissue sections. Briefly, 5-μm-thick sections were obtained with a microtome, transferred onto adhesive slides, and dried at 62°C for 30 minutes. After incubation with primary antibodies, immunodetection was performed with biotinylated anti-mouse immunoglobulin, followed by peroxidase-labeled streptavidin using a labeled streptavidin biotin kit with 3,3'-diaminobenzidine chromogen as the substrate. The primary antibody incubation step was omitted in the negative control. Slides were counterstained with Harris hematoxylin.

Interpretation of immunohistochemical staining

All immunohistochemical markers were assessed by light microscopy. The IHC stain results for androgen receptor (AR), cytokeratin (CK) 5/6, interleukin (IL)-8, signal transducer and activator of transcription (STAT)-1 and gamma-glutamyltransferase (GGT)-1 were considered positive when more than 10% of the tumor cells were stained. The IHC stain results for epidermal growth factor receptor (EGFR), claudin-3, claudin-4, claudin-7 and E-cadherin were classified into negative, weak, moderate and

Table 3. Clinicopathologic features according to subtype of TNBC

Parameter	Total *N*=129 (%)	Basal-like type *n*=54 (%)	Molecular apocrine type *n*=11 (%)	Claudin-low type *n*=8 (%)	Immune-related type n=6 (%)	Mixed type *n*=28 (%)	Null type *n*=22 (%)	*P*-value
Age (years, mean±SD)	48.5±12.5	47.0±11.3	51.3±15.4	49.8±8.2	52.3±18.7	49.3±12.9	48.4±13.4	0.843
Histologic grade								0.396
I	3 (2.3)	0 (0.0)	0 (0.0)	0 (0.0)	0 (0.0)	2 (7.1)	1 (4.5)	
II	37 (28.7)	16 (29.6)	6 (54.5)	3 (37.5)	1 (16.7)	7 (25.0)	4 (18.2)	
III	89 (69.0)	38 (70.4)	5 (45.5)	5 (62.5)	5 (83.3)	19 (67.9)	17 (77.3)	
Tumor stage								0.550
T1	49 (38.0)	24 (44.4)	5 (45.5)	3 (37.5)	1 (16.7)	9 (32.1)	7 (31.8)	
T2	78 (60.5)	29 (53.7)	5 (45.5)	5 (62.5)	5 (83.3)	19 (67.9)	15 (68.2)	
T3	2 (1.6)	1 (1.9)	1 (9.1)	0 (0.0)	0 (0.0)	0 (0.0)	0 (0.0)	
Nodal stage								0.950
N0	85 (65.9)	40 (74.1)	6 (54.5)	5 (83.3)	5 (83.3)	17 (60.7)	12 (54.5)	
N1	34 (26.4)	10 (18.5)	4 (36.4)	3 (37.5)	1 (16.7)	8 (28.6)	8 (36.4)	
N2	7 (5.4)	3 (5.6)	1 (9.1)	0 (0.0)	0 (0.0)	2 (7.1)	1 (4.5)	
N3	3 (2.3)	1 (1.9)	0 (0.0)	0 (0.0)	0 (0.0)	1 (3.6)	1 (4.5)	
Central acellular zone								0.216
No	98 (76.0)	37 (68.5)	11 (100.0)	6 (75.0)	6 (100.0)	21 (75.0)	17 (77.3)	
Yes	31 (24.0)	17 (31.5)	0 (0.0)	2 (25.0)	0 (0.0)	7 (25.0)	5 (22.7)	
Central necrotic zone								0.874
No	120 (93.0)	50 (92.6)	11 (100.0)	7 (87.5)	6 (100.0)	26 (92.9)	20 (90.9)	
Yes	9 (7.0)	4 (7.4)	0 (0.0)	1 (12.5)	0 (0.0)	2 (7.1)	2 (9.1)	
Central fibrotic zone								0.346
No	103 (79.8)	40 (74.1)	11 (100.0)	6 (75.0)	6 (100.0)	22 (78.6)	18 (81.8)	
Yes	26 (20.2)	14 (25.9)	0 (0.0)	2 (25.0)	0 (0.0)	6 (21.4)	4 (18.2)	
Lymphocytic infiltration								0.035
No	97 (75.2)	40 (74.1)	8 (72.7)	7 (87.5)	2 (33.3)	19 (67.9)	21 (95.5)	
Yes	32 (24.8)	14 (25.9)	3 (27.3)	1 (12.5)	4 (66.7)	9 (32.1)	1 (4.5)	
Tumor cell discohesiveness								0.096
No	120 (93.0)	52 (96.3)	8 (72.7)	7 (87.5)	6 (100.0)	27 (96.4)	20 (90.9)	
Yes	9 (7.0)	2 (3.7)	3 (27.3)	1 (12.5)	0 (0.0)	1 (3.6)	2 (9.1)	
Tumor margin								0.294
Expanding	110 (85.3)	48 (88.9)	8 (72.7)	7 (87.5)	6 (100.0)	25 (89.3)	16 (72.7)	
Infiltrative	19 (14.7)	6 (11.1)	3 (27.3)	1 (12.5)	0 (0.0)	3 (10.7)	6 (27.3)	
Apocrine differentiation								0.031
No	105 (81.4)	46 (85.2)	5 (45.5)	7 (87.5)	4 (66.7)	23 (82.1)	20 (90.9)	
Yes	24 (18.6)	8 (14.8)	6 (54.5)	1 (12.5)	2 (33.3)	5 (17.9)	2 (9.1)	
Ki-67 LI (%, mean±SD)	28.1±23.4	33.5±24.8	6.0±4.8	27.3±27.8	38.6±27.5	29.5±22.1	21.6±17.3	0.006

LI, labeling index; TNBC, triple-negative breast carcinoma.

Table 4. Metabolic phenotypes according to subtype of TNBC

Parameter	Total *N*=129 (%)	Basal-like type *n*=54 (%)	Molecular apocrine type *n*=11 (%)	Claudin-low type *n*=8 (%)	Immune-related type n=6 (%)	Mixed type *n*=28 (%)	Null type *n*=22 (%)	*P*-value
Tumoral phenotype								0.301
Glycolysis type	69 (53.5)	34 (63.0)	4 (36.4)	4 (50.0)	3 (50.0)	16 (57.1)	8 (36.4)	
Non-glycolysis type	60 (46.5)	20 (37.0)	7 (63.6)	4 (50.0)	3 (50.0)	12 (42.9)	14 (63.6)	
Stromal phenotype								0.385
Glycolysis type	21 (16.3)	10 (18.5)	0 (0.0)	1 (12.5)	0 (0.0)	7 (25.0)	3 (13.6)	
Non-glycolysis type	108 (83.7)	44 (81.5)	11 (100.0)	7 (87.5)	6 (100.0)	21 (75.0)	19 (86.4)	
Tumoral phenotype								0.496
Glutaminolysis type	87 (67.4)	37 (68.5)	5 (45.5)	5 (65.5)	3 (50.0)	21 (75.0)	16 (72.7)	
Non-glutaminolysis type	42 (32.6)	17 (31.5)	6 (54.5)	3 (37.5)	3 (50.0)	7 (25.0)	6 (27.3)	
Stromal phenotype								0.545
Glutaminolysis type	48 (37.2)	17 (31.5)	4 (36.4)	5 (62.5)	3 (50.0)	12 (42.9)	7 (31.8)	
Non-glutaminolysis type	81 (62.8)	37 (68.5)	7 (63.6)	3 (37.5)	3 (50.0)	16 (57.1)	15 (68.2)	
Tumoral phenotype								0.303
Mitochondrial type	110 (85.3)	48 (88.9)	8 (72.7)	7 (87.5)	4 (66.7)	26 (92.9)	17 (77.3)	
Non-mitochondrial type	19 (14.7)	6 (11.1)	3 (27.3)	1 (12.5)	2 (33.3)	2 (7.1)	5 (22.7)	
Stromal phenotype								0.577
Mitochondrial type	18 (14.0)	10 (18.5)	2 (18.2)	0 (0.0)	0 (0.0)	4 (14.3)	2 (9.1)	
Non-mitochondrial type	111 (86.0)	44 (81.5)	9 (81.8)	8 (100.0)	6 (100.0)	24 (85.7)	20 (90.9)	

TNBC, triple-negative breast carcinoma.

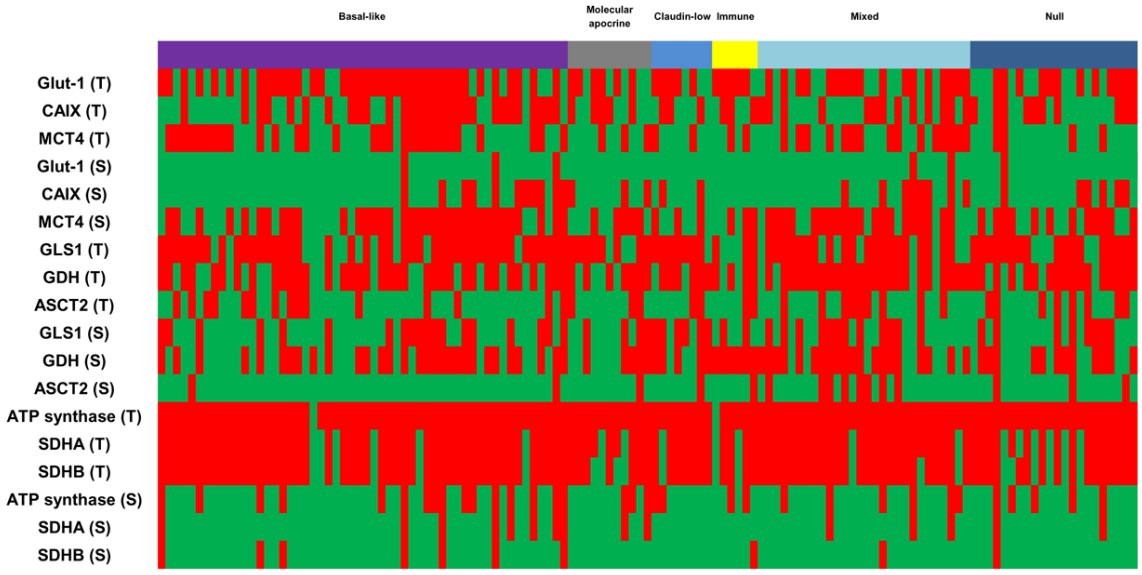

Figure 1. A heat map of immunohistochemical results of metabolism-related proteins according to the molecular subtype of TNBC. T tumor, S stroma, Red positive, Green negative.

intense expression. The cases with moderate or intense expression were considered positive. The assessment of immunohistochemical staining of metabolism-related proteins was based on the product of the proportion of stained cells and the immunostaining intensity. The grades of the proportion of stained cells were 0: negative, 1: <30% of positive cells, and 2: ≥30% of positive cells, while the grades of immunostaining intensity were 0: negative, 1: weak, 2: moderate, and 3, strong. The product of the proportion of stained cells and the immunostaining intensity was judged as negative for 0-1, weakly positive for 2-4, and highly positive for 5-6. Results for Ki-67 were scored by counting the positively stained nuclei and expressing this number as a percentage of the total tumor cell number [Ki-67 labeling index (LI)].

Molecular classification of TNBC according to IHC

According to the results of IHC, TNBC was subclassified into *basal-like type* (CK5/6-positive and/or EGFR-positive), *molecular apocrine type* (AR-positive and/or GGT-1-positive), *claudin-low type* (claudin 3-, claudin 4-, claudin 7-negative and/or E-cadherin-negative), immune-related type (IL-8-negative and stromal STAT1-positive), *mixed type* (two or more types), and null type (none of these).

Metabolic classification of TNBC according to IHC

Metabolic phenotypes were classified as follows, based on the expression of metabolism-related proteins: *glycolysis type* (positive for two or more of Glut-1, CAIX and MCT-4), *glutaminolysis type* (positive for two or more of GLS1, GDH and ASCT2), and *mitochondrial type* (positive for two or more of ATP synthase, SDHA and SDHB).

Statistical analysis

Data were processed using SPSS for Windows, version 12.0 (SPSS Inc., Chicago, IL, USA). Student's *t* and Fisher's exact tests were used to examine any difference in continuous and categorical variables, respectively. The limit for statistical significance was set at P=0.05. Kaplan-Meier survival curves and log-rank statistics were employed to evaluate time to tumor metastasis and time to survival. Multivariate regression analysis was performed using Cox proportional hazards model.

Results

Clinicopathologic characteristics of TNBC

The most common type of TNBC was basal-like type (54%), followed by molecular apocrine type (11%), claudin-low type (8%), and immune-relat-

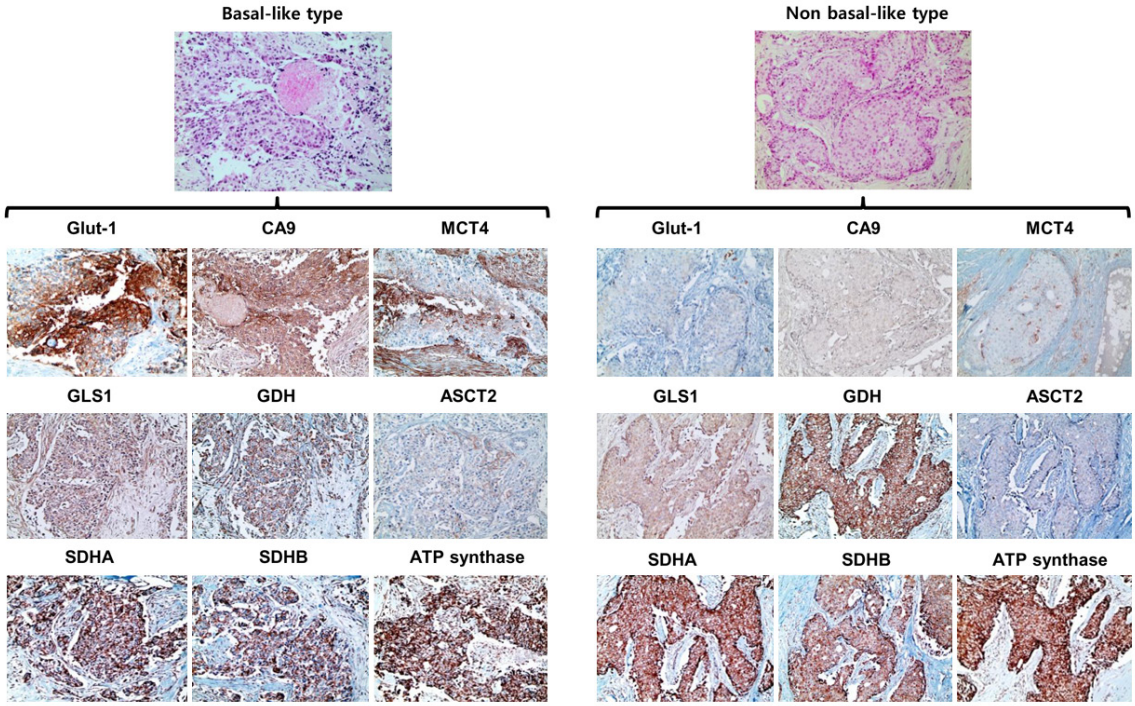

Figure 2. Immunohistochemical expression of metabolism-related proteins in basal-like and non-basal-like TNBC. The expression of glycolysis-related proteins is high in basal-like type, while the expression is low in non-basal-like type.

Table 5. Comparison of metabolic phenotypes between basal-like type and non-basal-like type

Parameter	Basal-like type n=79 (%)	Non-basal-like type n=50 (%)	*p*-value
Tumoral phenotype			0.047
Glycolysis type	48 (60.8)	21 (42.0)	
Non-glycolysis type	31 (39.2)	29 (58.0)	
Stromal phenotype			0.148
Glycolysis type	16 (20.3)	5 (10.0)	
Non-glycolysis type	63 (79.7)	45 (90.0)	
Tumoral phenotype			0.565
Glutaminolysis type	55 (69.6)	32 (64.0)	
Non-glutaminolysis type	24 (30.4)	18 (36.0)	
Stromal phenotype			0.455
Glutaminolysis type	27 (34.2)	21 (42.0)	
Non-glutaminolysis type	52 (65.8)	29 (58.0)	
Tumoral phenotype			0.077
Mitochondrial type	71 (89.9)	39 (78.0)	
Non-mitochondrial type	8 (10.1)	11 (22.0)	
Stromal phenotype			0.191
Mitochondrial type	14 (17.7)	4 (8.0)	
Non-mitochondrial type	65 (82.3)	46 (92.0)	

ed type (6%). In addition, there was mixed type (28%) and null type (22%). Lymphocytic infiltration was highest in the immune-related type and lowest in the null type (p=0.035), while apocrine differentiation was most commonly observed in the molecular apocrine type but rarely in the null type (p=0.031). Ki-67 labeling index was highest in immune-related type and lowest in molecular apocrine type (p=0.006, **Table 3**).

Metabolic phenotypes according to molecular subtype of TNBC

The analysis of metabolic phenotypes of tumor and stroma based on molecular subtypes of TNBC suggested no statistically significant difference, but tumors of basal-like type showed a higher ratio of glycolysis type, while tumors of molecular apocrine type and null type showed a higher ratio of non-glycolysis type, and stroma of claudin-low type showed a higher ratio of glutaminolysis type (**Table 4**). A heat map of immunohistochemical results formetabolism-related proteins is shown in **Figure 1**.

Table 6. Clinicopathologic characteristics according to the metabolic phenotype in tumor and stroma

Parameter	Tumoral phenotype			Stromal phenotype			Tumoral phenotype			Stromal phenotype			Tumoral phenotype			Stromal phenotype		
	Glycolysis type n=69 (%)	Non-glycolysis type n=60 (%)	*P-value**	Glycolysis type	Non-glycolysis type	*P-value**	Glutaminolysis type	Non-glutaminolysis type	*P-value**	Glutaminolysis type	Non-glutaminolysis type	*P-value**	Mitochondrial type	Non-mitochondrial type	*P-value**	Mitochondrial type	Non-mitochondrial type	*P-value**
Age (years)			4.926			2.166			2.838			1.452			3.144			4.464
≤35	12 (17.4)	12 (20.0)		2 (9.5)	22 (20.4)		18 (20.7)	6 (14.3)		6 (12.5)	18 (22.2)		22 (20.0)	2 (10.5)		4 (22.2)	20 (18.0)	
>35	57 (82.6)	48 (80.0)		19 (90.5)	86 (79.6)		69 (79.3)	36 (85.7)		42 (87.5)	63 (77.8)		88 (80.0)	17 (89.5)		14 (77.8)	91 (82.0)	
Histologic grade			0.120			4.806			2.550			6.000			1.074			2.550
I/II	15 (21.7)	25 (41.7)		7 (33.3)	33 (30.6)		25 (28.7)	15 (35.7)		15 (31.3)	25 (30.9)		37 (33.6)	3 (15.8)		7 (38.9)	33 (29.7)	
III	54 (78.3)	35 (58.3)		14 (66.7)	75 (69.4)		62 (71.3)	27 (64.3)		33 (68.8)	56 (69.1)		73 (66.4)	16 (84.2)		11 (61.1)	78 (70.3)	
Tumor stage			5.136			0.894			2.670			0.234			0.054			0.222
T1	27 (39.1)	22 (36.7)		11 (52.4)	38 (35.2)		31 (35.6)	18 (42.9)		24 (50.0)	25 (30.9)		47 (42.7)	2 (10.5)		11 (61.1)	38 (34.2)	
T2/T3	42 (60.9)	38 (63.3)		10 (47.6)	70 (64.8)		56 (64.4)	24 (57.1)		24 (50.0)	56 (69.1)		63 (57.3)	17 (89.5)		7 (38.9)	73 (65.8)	
Nodal stage			0.102			4.812			1.416			3.408			3.612			4.734
N0	52 (75.4)	33 (55.0)		13 (61.9)	72 (66.7)		54 (62.1)	31 (73.8)		30 (62.5)	55 (67.9)		71 (64.5)	14 (73.7)		11 (61.1)	74 (66.7)	
N1/N2/N3	17 (24.6)	27 (45.0)		8 (38.1)	36 (33.3)		33 (37.9)	11 (26.2)		18 (37.5)	26 (32.1)		39 (35.5)	5 (26.3)		7 (38.9)	37 (33.3)	
Lymphocytic infiltration			5.034			1.676			0.792			5.004			6.000			1.428
Absent	51 (73.9)	46 (76.7)		18 (85.7)	79 (73.1)		69 (79.3)	28 (66.7)		37 (77.1)	60 (74.1)		83 (75.5)	14 (73.7)		16 (88.9)	81 (73.0)	
Present	18 (26.1)	14 (23.3)		3 (14.3)	29 (26.9)		18 (20.7)	14 (33.3)		11 (22.9)	21 (25.9)		27 (24.5)	5 (26.3)		2 (11.1)	30 (27.0)	
Tumor cell discohesiveness			0.072			2.124			2.826			4.356			6.000			6.000
No	68 (98.6)	52 (86.7)		21 (100)	99 (91.7)		82 (94.3)	38 (90.5)		44 (91.7)	76 (93.8)		102 (92.7)	18 (94.7)		17 (94.4)	103 (92.8)	
Yes	1 (1.4)	8 (13.3)		0 (0.0)	9 (8.3)		5 (5.7)	4 (9.5)		4 (8.3)	5 (6.2)		8 (7.3)	1 (5.3)		1 (5.6)	8 (7.2)	
Tumor margin			0.282			4.422			2.562			6.000			6.000			1.824
Expanding	63 (91.3)	47 (78.3)		19 (90.5)	91 (84.3)		76 (87.4)	34 (81.0)		41 (85.4)	69 (85.2)		94 (85.5)	16 (84.2)		14 (77.8)	96 (86.5)	
Infiltrative	6 (8.7)	13 (21.7)		2 (9.5)	17 (15.7)		11 (12.6)	8 (19.0)		7 (14.6)	12 (14.8)		16 (14.5)	3 (15.8)		4 (22.2)	15 (13.5)	
Apocrine differentiation			4.926			3.252			3.786			3.870			4.524			6.000
No	57 (82.6)	48 (80.0)		16 (76.2)	89 (82.4)		72 (82.8)	33 (78.6)		38 (79.2)	67 (82.7)		90 (81.8)	15 (78.9)		15 (83.3)	90 (81.1)	
Yes	12 (17.4)	12 (20.0)		5 (23.8)	19 (17.6)		15 (17.2)	9 (21.4)		10 (20.8)	14 (17.3)		20 (18.2)	4 (21.1)		3 (16.7)	21 (18.9)	
Ki-67 LI (%, mean±SD)	29.9±23.6	26.1±23.1	2.142	31.7±19.1	27.4±24.1	2.664	26.6±22.9	31.2±24.3	1.812	33.8±25.6	24.8±21.4	0.204	29.2±23.4	21.9±22.8	1.272	29.9±23.1	27.8±23.5	4.374

**p*-value was adjusted by Bonferroni correction.

Table 7. Univariate analysis of the metabolic phenotypes in TNBC and disease-free survival or overall survival by log-rank test

Parameter	Number of patients/ recurrence/death	Disease-free survival		Overall survival	
		Mean survival (95% CI) months	*P*-value	Mean survival (95% CI) months	*P*-value
Tumoral phenotype			0.636		0.126
Glycolysis type	69/6/4	94 (89-100)		97 (93-102)	
Non-glycolysis type	60/7/9	91 (84-98)		89 (81-96)	
Stromal phenotype			0.421		0.463
Glycolysis type	21/1/1	63 (59-66)		64 (62-65)	
Non-glycolysis type	108/12/12	92 (87-98)		93 (88-98)	
Tumoral phenotype			0.377		0.721
Glutaminolysis type	87/10/9	91 (85-98)		92 (86-98)	
Non-glutaminolysis type	42/3/4	95 (89-101)		93 (86-100)	
Stromal phenotype			0.144		0.470
Glutaminolysis type	48/2/3	94 (89-99)		92 (87-98)	
Non-glutaminolysis type	81/11/10	91 (84-97)		92 (87-98)	
Tumoral phenotype			0.435		0.455
Mitochondrial type	110/10/10	94 (89-99)		94 (89-99)	
Non-mitochondrial type	19/3/3	84 (71-98)		86 (74-97)	
Stromal phenotype			0.847		0.774
Mitochondrial type	18/2/2	73 (63-82)		74 (65-82)	
Non-mitochondrial type	111/11/11	93 (88-98)		94 (89-98)	

When the metabolic phenotype of TNBC was investigated between basal-like type and non-basal-like type, a difference in glycolysis status was observed; the glycolysis type was higher in the basal-like type of tumor, while non-glycolysis type was higher in the non-basal-like type (p=0.047). In the mitochondrial type of tumor, basal-like type was more frequent than non-basal-like type (p=0.077, **Table 5**).

Correlation of metabolic phenotypes in tumor and stroma

The analysis of metabolic phenotypes of tumor and stroma suggested significant correlation between glycolysis and mitochondrial type of stroma (p<0.001), glutaminolysis and mitochondrial type of stroma (p<0.001), and glutaminolysis and mitochondrial type of tumor (p<0.001) (**Figure 2**).

Clinicopathologic characteristics according to the metabolic phenotype in tumor and stroma

The analysis of correlation between metabolic phenotypes of tumor and stroma and clinicopathologic characteristics suggested that tumor cell discohesiveness was increased, though not statistically significant, in non-glycolysis type (p=0.072), and the mitochondrial type of tumor showed lower T stage (p=0.054, **Table 6**).

The analysis of correlation between metabolic phenotypes and disease-free survival (DFS) and overall survival (OS) found no statistically significant factors (**Table 7**).

Discussion

In this study, we investigated the expression patterns of proteins related to cancer metabolism including glycolysis, glutaminolysis and mitochondrial metabolism. The analysis of metabolic phenotypes based on surrogate IHC suggested that the most common metabolic phenotype of TNBC are mitochondrial type (85.3%), followed by glutaminolysis type (67.4%), and glycolysis type (63.0%). The well-known Warburg effect [14] involves a metabolic shift from mitochondrial oxidative phosphorylation to aerobic glycolysis. In this study, cancer cells of TNBC showed a higher ratio of mitochondrial type to glycolysis type. A previous study reported that the predominant energy metabolism takes different forms such as glycolysis or oxidative phosphorylation depending on tumor

cell type [9]. As for breast cancer, there have been varying reports on the predominant energy metabolism, from oxidative phosphorylation [15] to glycolysis and oxidative phosphorylation [16]. A gene signature study also reported a high correlation between glycolysis- and oxidative-phosphorylation-related signature and proliferation [17]. As TNBC is a representative of highly aggressive tumors with proliferative activity, both glycolysis and oxidative phosphorylation of cancer cell metabolism could be expected, which is supported by the results of this study. In this study, there was no significant difference in metabolic phenotype based on molecular subtype by surrogate IHC. However, this could result from the difficulties in accurate analysis due to the limited numbers of each subtype, suggesting that an extended study is required with larger numbers of samples. When TNBC is classified into basal-like type and non-basal-like type, however, the ratio of glycolysis type was higher in basal-like type of tumor, while that of non-glycolysis type was higher in non-basal-like type. It was reported that the expression of glycolysis-related proteins such as Glut-1, CAIX and MCT4 was higher in the basal-like phenotype of breast cancer [18-20], which is consistent with the results of this study. It should be noted that the metabolic phenotype was observed in the stroma and was not limited to the tumor. The most common metabolic phenotype of stroma was glutaminolysis type (37.2%), followed by glycolysis type (16.3%) and mitochondrial type (14.0%). Based on the molecular subtypes, non-glycolysis type was observed in all stroma of molecular apocrine type, while non-mitochondrial type was observed in those of claudin-low type, and non-glycolysis type and non-mitochondrial type were observed in those of immune-related type. These results imply that there are different profiles for the molecular subtypes, but this finding should be interpreted with caution due to the limited numbers of each subtype. The interaction between tumor and stroma plays an important role in the growth and progression of tumors. The interaction can also be important in view of metabolism. One of the hypotheses about metabolic interaction between tumor and stroma in breast cancer is the reverse Warburg effect [21]. This theory can be summarized as follow: breast cancer cells generate reactive oxygen species (ROS) such as nitric oxide (NO), which serve as oxidative stress to stromal cells through HIF-1α and NF-κB, leading to glycolysis, autophagy (mitophagy), and mitochondrial dysfunction. The ketone bodies and lactate produced by glycolysis in stromal cells enter the cancer cells and effectively produce ATP by oxidative phosphorylation in the mitochondria, contributing to the survival and growth of the cancer cells. Therefore, stromal cells show glycolysis type, while tumor cells show mitochondrial type in the reverse Warburg effect theory. In addition, a metabolic interaction for glutamine metabolism in the tumor and stroma is suggested. This vicious cycle can be described as follows: ammonia, a byproduct of tumor cell glutaminolysis, diffuses into the stroma where it induces autophagy, followed by generation of glutamine as a product of autophagy activity, which is transported back to tumor cells [22-26]. Glutamine uptake molecules and glutaminase are mainly expressed in cancer cells, while the expression of glutamine synthetase is mostly observed in stromal cells [26]. We also found various metabolic phenotypes of the stroma as well as tumor, which require further studies. In the analysis of correlation between metabolic phenotypes of tumor and stroma, we found significant correlation between glutaminolysis type and mitochondrial type of both tumor and stroma. As α-ketoglutarate generated by glutaminolysis can be used as a mitochondrial substrate, a relationship between glutaminolysis and mitochondrial enzymes could be expected [27] and was demonstrated in this study.

In this study, metabolic activity was evaluated based on the expression of metabolism-related proteins, but more accurate evaluation can be obtained through the investigation of metabolic flux. However, the metabolic flux cannot be measured using paraffin-embedded human tissue samples, and thus the expression of metabolism-related proteins was measured by IHC as a surrogate method. Such metabolic phenotypes of TNBC can be clinically implicated as a possible targeted therapy. As TNBC is negative for all ER, PR and HER-2, there are no efficient targeted therapies at present. Glycolysis inhibitors, glutamine metabolism inhibitors, and other metabolism-related proteins are under preclinical study as possible targeted therapies [28, 29]. Therefore, metabolic phenotypes may play a crucial role in future targeted therapies. In conclusion, TNBC

shows the expression of both glycolysis- and mitochondrial metabolism-related proteins in tumor cells with higher ratios of glycolysis type in basal-like type tumors and non-glycolysis type in non-basal-like type tumors.

Acknowledgements

This research was supported by the Basic Science Research Program through the National Research Foundation of Korea (NRF), funded by the Ministry of Education, Science and Technology (2012R1A1A1002886); and by a faculty research grant from Yonsei University College of Medicine for 2013 (6-2013-0146).

Disclosure of conflict of interest

The authors declare that they have no competing interests.

Address correspondence to: Dr. Ja Seung Koo, Department of Pathology, Yonsei University College of Medicine, Severance Hospital, 50 Yonsei-Ro, Seodaemun-Gu, Seoul, 120-752, South Korea. Tel: 82-2-2228-1772; Fax: 82-2-362-0860; E-mail: kjs1976@yuhs.ac

References

[1] Perou CM, Sorlie T, Eisen MB, van de Rijn M, Jeffrey SS, Rees CA, Pollack JR, Ross DT, Johnsen H, Akslen LA, Fluge O, Pergamenschikov A, Williams C, Zhu SX, Lonning PE, Borresen-Dale AL, Brown PO and Botstein D. Molecular portraits of human breast tumours. Nature 2000; 406: 747-752.

[2] Sørlie T, Perou CM, Tibshirani R, Aas T, Geisler S, Johnsen H, Hastie T, Eisen MB, van de Rijn M, Jeffrey SS, Thorsen T, Quist H, Matese JC, Brown PO, Botstein D, Lønning PE, Børresen-Dale AL. Gene expression patterns of breast carcinomas distinguish tumor subclasses with clinical implications. Proc Natl Acad Sci U S A 2001; 98: 10869-10874.

[3] Dent R, Trudeau M, Pritchard KI, Hanna WM, Kahn HK, Sawka CA, Lickley LA, Rawlinson E, Sun P and Narod SA. Triple-negative breast cancer: clinical features and patterns of recurrence. Clin Cancer Res 2007; 13: 4429-4434.

[4] Perou CM. Molecular stratification of triple-negative breast cancers. Oncologist 2011; 16 Suppl 1: 61-70.

[5] Reis-Filho JS and Tutt AN. Triple negative tumours: a critical review. Histopathology 2008; 52: 108-118.

[6] Foulkes WD, Smith IE and Reis-Filho JS. Triple-negative breast cancer. N Engl J Med 2010; 363: 1938-1948.

[7] Pollard PJ, Wortham NC and Tomlinson IP. The TCA cycle and tumorigenesis: the examples of fumarate hydratase and succinate dehydrogenase. Ann Med 2003; 35: 632-639.

[8] Rakha EA and Ellis IO. Triple-negative/basal-like breast cancer: review. Pathology 2009; 41: 40-47.

[9] Korpershoek E, Favier J, Gaal J, Burnichon N, van Gessel B, Oudijk L, Badoual C, Gadessaud N, Venisse A, Bayley JP, van Dooren MF, de Herder WW, Tissier F, Plouin PF, van Nederveen FH, Dinjens WN, Gimenez-Roqueplo AP and de Krijger RR. SDHA immunohistochemistry detects germline SDHA gene mutations in apparently sporadic paragangliomas and pheochromocytomas. J Clin Endocrinol Metab 2011; 96: E1472-1476.

[10] Hamele-Bena D, Cranor ML and Rosen PP. Mammary mucocele-like lesions. Benign and malignant. Am J Surg Pathol 1996; 20: 1081-1085.

[11] Hammond ME, Hayes DF, Dowsett M, Allred DC, Hagerty KL, Badve S, Fitzgibbons PL, Francis G, Goldstein NS, Hayes M, Hicks DG, Lester S, Love R, Mangu PB, McShane L, Miller K, Osborne CK, Paik S, Perlmutter J, Rhodes A, Sasano H, Schwartz JN, Sweep FC, Taube S, Torlakovic EE, Valenstein P, Viale G, Visscher D, Wheeler T, Williams RB, Wittliff JL and Wolff AC. American Society of Clinical Oncology/College Of American Pathologists guideline recommendations for immunohistochemical testing of estrogen and progesterone receptors in breast cancer. J Clin Oncol 2010; 28: 2784-2795.

[12] Wolff AC, Hammond ME, Schwartz JN, Hagerty KL, Allred DC, Cote RJ, Dowsett M, Fitzgibbons PL, Hanna WM, Langer A, McShane LM, Paik S, Pegram MD, Perez EA, Press MF, Rhodes A, Sturgeon C, Taube SE, Tubbs R, Vance GH, van de Vijver M, Wheeler TM and Hayes DF. American Society of Clinical Oncology/College of American Pathologists guideline recommendations for human epidermal growth factor receptor 2 testing in breast cancer. J Clin Oncol 2007; 25: 118-145.

[13] Elston CW and Ellis IO. Pathological prognostic factors in breast cancer. I. The value of histological grade in breast cancer: experience from a large study with long-term follow-up. Histopathology 1991; 19: 403-410.

[14] Warburg O. On the origin of cancer cells. Science 1956; 123: 309-314.

[15] Gottlieb E and Tomlinson IP. Mitochondrial tumour suppressors: a genetic and biochemical update. Nat Rev Cancer 2005; 5: 857-866.

[16] Hanski C, Hofmeier M, Schmitt-Graff A, Riede E, Hanski ML, Borchard F, Sieber E, Niedobitek F, Foss HD, Stein H and Riecken EO. Overexpression or ectopic expression of MUC2 is the common property of mucinous carcinomas of the colon, pancreas, breast, and ovary. J Pathol 1997; 182: 385-391.

[17] Harris JR, Lippman ME, Morrow M and Osborne KC. Diseases of the breast. In: editors. Philadelphia: Lippincott Williams & Wilkin; 2004. pp: 253.

[18] Gomez I, Pena C, Herrera M, Munoz C, Larriba MJ, Garcia V, Dominguez G, Silva J, Rodriguez R, Garcia de Herreros A, Bonilla F and Garcia JM. TWIST1 is expressed in colorectal carcinomas and predicts patient survival. PLoS One 2011; 6: e18023.

[19] Pinheiro C, Sousa B, Albergaria A, Paredes J, Dufloth R, Vieira D, Schmitt F and Baltazar F. GLUT1 and CAIX expression profiles in breast cancer correlate with adverse prognostic factors and MCT1 overexpression. Histol Histopathol 2011; 26: 1279-1286.

[20] Tan EY, Yan M, Campo L, Han C, Takano E, Turley H, Candiloro I, Pezzella F, Gatter KC, Millar EK, O'Toole SA, McNeil CM, Crea P, Segara D, Sutherland RL, Harris AL and Fox SB. The key hypoxia regulated gene CAIX is upregulated in basal-like breast tumours and is associated with resistance to chemotherapy. Br J Cancer 2009; 100: 405-411.

[21] Pavlides S, Whitaker-Menezes D, Castello-Cros R, Flomenberg N, Witkiewicz AK, Frank PG, Casimiro MC, Wang C, Fortina P, Addya S, Pestell RG, Martinez-Outschoorn UE, Sotgia F and Lisanti MP. The reverse Warburg effect: aerobic glycolysis in cancer associated fibroblasts and the tumor stroma. Cell Cycle 2009; 8: 3984-4001.

[22] Kang Y and Massague J. Epithelial-mesenchymal transitions: twist in development and metastasis. Cell 2004; 118: 277-279.

[23] Lee TK, Poon RT, Yuen AP, Ling MT, Kwok WK, Wang XH, Wong YC, Guan XY, Man K, Chau KL and Fan ST. Twist overexpression correlates with hepatocellular carcinoma metastasis through induction of epithelial-mesenchymal transition. Clin Cancer Res 2006; 12: 5369-5376.

[24] Li A, Goto M, Horinouchi M, Tanaka S, Imai K, Kim YS, Sato E and Yonezawa S. Expression of MUC1 and MUC2 mucins and relationship with cell proliferative activity in human colorectal neoplasia. Pathol Int 2001; 51: 853-860.

[25] Libura J, Drukala J, Majka M, Tomescu O, Navenot JM, Kucia M, Marquez L, Peiper SC, Barr FG, Janowska-Wieczorek A and Ratajczak MZ. CXCR4-SDF-1 signaling is active in rhabdomyosarcoma cells and regulates locomotion, chemotaxis, and adhesion. Blood 2002; 100: 2597-2606.

[26] Ko YH, Lin Z, Flomenberg N, Pestell RG, Howell A, Sotgia F, Lisanti MP and Martinez-Outschoorn UE. Glutamine fuels a vicious cycle of autophagy in the tumor stroma and oxidative mitochondrial metabolism in epithelial cancer cells: Implications for preventing chemotherapy resistance. Cancer Biol Ther 2011; 12: 1085-1097.

[27] Kovacevic Z. The pathway of glutamine and glutamate oxidation in isolated mitochondria from mammalian cells. Biochem J 1971; 125: 757-763.

[28] Dang CV, Hamaker M, Sun P, Le A and Gao P. Therapeutic targeting of cancer cell metabolism. J Mol Med (Berl) 2011; 89: 205-212.

[29] Wise DR and Thompson CB. Glutamine addiction: a new therapeutic target in cancer. Trends Biochem Sci 2010; 35: 427-433.